PHYSICAL REVIEW B VOLUME 58, NUMBER 3 15 JULY 1998-I

Stacking faults in group-IV crystals: An *ab initio* study

Peter Käckell, Jürgen Furthmüller, and Friedhelm Bechstedt
Institut für Festkörpertheorie und Theoretische Optik, Friedrich-Schiller-Universität, Max-Wien-Platz 1, 07743 Jena, Germany

(Received 24 February 1998)

Intrinsic and extrinsic stacking faults along the [111] direction in cubic SiC, Si, and C are studied within a first-principles scheme based on density-functional theory and the local-density approximation. In contrast to stacking fault energies for Si and C, we find them to be negative for SiC, possibly one part of the explanation for the large variety of hexagonal and rhombohedral polytypes. The formation energies are compared with experimental and theoretical data available and the chemical trends are derived for the geometrical changes. The electronic structure is calculated for the energetically favorable stacking faults in SiC.
[S0163-1829(98)01627-0]

It is a well-known fact that among materials crystallizing in a close-packed structure there are several showing a tendency to deviate from the rules of building their lattice by creating a stacking fault. Sometimes it happens that those deviations become a rule themselves. Then stacking faults are repeated periodically and a polytype is formed, which, of course, can be considered as a faultless structure with a large period and new translational symmetry.

From the materials showing polytypism, SiC is the most important example due to the large variety of stable polytypes actually observed. More than 200 polytypes of SiC are known. Furthermore, stacking faults play a crucial role for the mobility of dislocations.[1,2] In contrast to other defects like dislocations or vacancies, no bonds are broken and the energy differences are expected to be very small compared to the unfaulted structures. Hence it is rather difficult to calculate the stacking-fault energies accurately. Only a few attempts were made to study stacking faults with first-principles methods. Chou *et al.* calculated their formation energies, the atomic structure, and the accompanying electronic states for silicon.[3] Denteneer used a first-principles method to calculate the total energies for several polytypes[4] and extracted the stacking-fault energies for Si, C, and SiC from an ANNNI (axial next-nearest neighbor Ising) model.[5]

In this paper, we study the stacking faults in SiC, Si, and C, crystallizing in zinc-blende or diamond structure, within the scheme of density-functional theory (DFT) in the local-density approximation (LDA).[6,7] For the exchange-correlation energy, the data of Ceperley and Alder[8] in the parametrization of Perdew and Zunger[9] have been used. The electron-ion interaction is described with norm-conserving *ab initio* pseudopotentials of Bachelet-Hamann-Schlüter type[10] in the Kleinman-Bylander factorization.[11] The carbon pseudopotential has been modified slightly to allow a lower cutoff E_{cut} for the plane-wave basis-set.[12] Convergency is reached for SiC at $E_{\mathrm{cut}}=34$ Ry,[12,13] for Si at $E_{\mathrm{cut}}=20$ Ry, and for C at $E_{\mathrm{cut}}=42$ Ry.[14] Based on a method to study the structural properties of different SiC polytypes,[13] we derive the formation energies for the stacking faults. The deviations of the atomic positions in the faulted planes are obtained by relaxing the atoms according to vanishing Hellmann-Feynman forces. Finally, an interesting aspect in association with defects is the existence of electronic states within the fundamental gap, which is also investigated for the most favorable faults. The single-particle energies are identified with the solutions of the Kohn-Sham equations.

Generally, stacking faults represent irregularities in the otherwise perfect stacking sequence. However, the number of bonds remains unchanged, i.e., in the materials under consideration the tetrahedral coordination is not destroyed. Stacking faults in fcc crystals occur if the stacking sequence differs from the cubic close-packed one $\ldots ABCABC\ldots$ along the [111] direction. In crystals with zinc-blende or diamond structure actually the stacking is $AA'BB'CC'AA'BB'CC'$— every second layer is placed on top of the first layer with a separation equal to the bond length. The distance between neighbored atomic planes belonging to different bilayers, e.g., between A' and B, equals one-third of the bond length. Keeping the convention in mind that A,B,C shall denote a bilayer of the two atoms belonging to one unit cell, we can abbreviate the cubic stacking sequence with ABC. This sequence is repeated infinitely. Other polytypes have different stacking sequences to be repeated, like the hexagonal ones AB ($2H$, wurtzite), $ABCB(4H)$, or $ABCACB(6H)$.

The most common stacking faults in cubic materials are the intrinsic and extrinsic stacking faults (ISF and ESF) to which we will restrict the studies. The ISF can be thought of as *removing* one double layer from the infinite stacking sequence, for example, by condensation of vacancies. Another physical process generating an ISF is a plastic glide caused by shear stress applied to the crystal. The resulting stacking sequence is $\ldots ABCA/CABC\ldots$, if a double layer B is removed, as for instance shown in Fig. 1. The ESF on the other hand can be thought of *adding* a double layer to the stacking sequence, for example by the condensation of interstitials. The resulting stacking sequence in this case is $\ldots ABCA/C/BCABC\ldots$ (cf. Fig 1). Another interpretation of the occurrence of the stacking faults is related to a twist of the three equivalent bonds between two bilayers by 180°. Then, besides staggered (cubic) layers also eclipsed (hexagonal) bilayers appear.

The calculations of the stacking fault energies at zero temperature were performed within a Car-Parrinello-like moleculardynamic approach.[15,16] Within this method, atomic

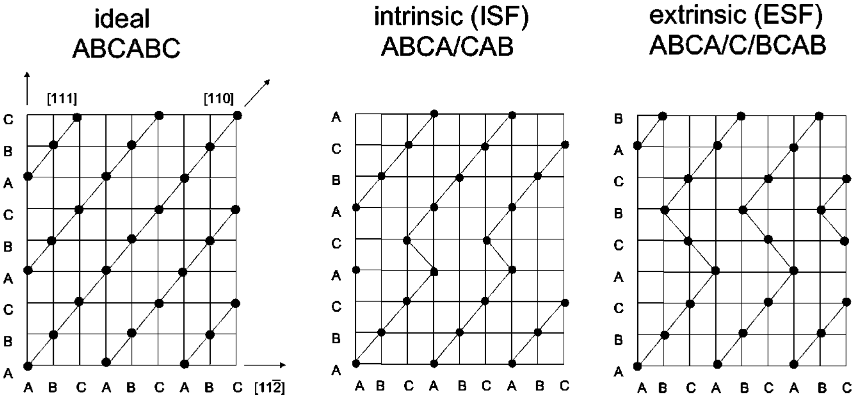

FIG. 1. Stacking sequences for an ideal fcc structure (left panel), fcc with ISF (middle panel), and fcc with ESF (right panel). A,B,C represent the three inequivalent positions within a $(1\bar{1}0)$ plane of a unit cell.

and electronic degrees of freedom are optimized simultaneously. The atoms (ions) are relaxed according to the Hellmann-Feynman forces until they vanish within the numerical accuracy (approximately 10^{-4} Å). The structure is simulated within a supercell approach. On the (111) plane the stacking fault therefore corresponds to an infinite planar defect as in reality. In the [111] direction the stacking fault is repeated after a certain number of double layers. Therefore we must assure that there are enough well-stacked double layers in the supercell to avoid interactions between the faulted layers.

For the calculations we use a repeated arrangement of supercells of hexagonal symmetry with the third axis (c) along the [111] direction. Supercells of the type $(5+3n)H$ ($n=0,1,2,\ldots$) or $(4+3m)H$ ($m=0,1,2,\ldots$) are possible for the description of ISF and ESF, respectively. The almost vanishing (artificial) interactions between stacking faults have been investigated by varying the supercell size. After careful tests of the convergency with respect to the energies and the atomic coordinates, we found unit cells containing eight ($n=1$) double layers for the ISF ($ABC/BCABC$) and seven ($m=1$) for the ESF ($AB/A/CABC$) (see Fig. 1) to be sufficient. However, for the calculation of the stacking-fault energies we have to compare with the total energies of unfaulted structures. Since the Brillouin zone integration is replaced by a summation over six special **k** points of Chadi-Cohen type,[17] one has to take special care that the calculations for faulted and unfaulted supercells are performed under equivalent conditions. For different cell sizes, this could be covered by equivalent sets of **k** points with respect to the sampling of the Brillouin zone. Another possibility is to represent faulted and unfaulted systems in supercells of the same size. The smallest unit for the unfaulted zinc-blende structure in the [111] direction consists of three double layers. Therefore, the supercell for the ISF must contain at least $8\times3=24$ bilayers, and, respectively, the supercell for the ESF $7\times3=21$ bilayers. The stacking fault energies themselves are finally obtained by subtracting the total energies of the two large-supercell calculations from each other, which is expected to cancel most of the systematic failures of the calculational method.

The one-dimensional character of the stacking difference in polytypes and periodic arrangement of ISF/ESF supercells suggests a description within the ANNNI model, where the ith cubic (hexagonal) bilayer is represented by a pseudospin up $\sigma_i=+1$ (down $\sigma_i=-1$). Neglecting interactions with more than two spins involved, the total energy per Si-C pair of a nH supercell arrangement can be written as

$$E=E_0-\frac{1}{n}\sum_{i=1}^{n}\sum_{j=1}^{\infty}J_j\sigma_i\sigma_{i+j}, \tag{1}$$

where j runs over the interacting bilayers and E_0 is an energy independent of the bilayer stacking.

Restricting the interactions on not more than between third-nearest neighbors, the total energies of only four stacking sequences—for instance, of the four polytypes $3C$, $2H$, $4H$, and $6H$—have to be calculated by a first-principles method to determine the three interaction parameters J_1, J_2, and J_3 as well as the energy E_0. This has been widely done for silicon carbide,[4,5,18–20] but also for Si and C restricting to second-nearest-neighbor interaction.[4,20] The energy representation (1) also allows the calculations of the formation energy $\Delta E_{\mathrm{ISF/ESF}}$ of a stacking fault per one atom in a two-dimensional unit cell perpendicular to the c axis. One finds

$$\Delta E_{\mathrm{ISF}}=4J_1+4J_2+4J_3,\quad \Delta E_{\mathrm{ESF}}=4J_1+8J_2+8J_3. \tag{2}$$

The stacking-fault energies $\gamma_{\mathrm{ISF/ESF}}$ per unit area follow from $\Delta E_{\mathrm{ISF/ESF}}$ by division with the area $\sqrt{3}a_0^2/4$ of one atom in a (111) plane. For the cubic lattice constant we use the theoretical values $a_0=4.29$ Å (SiC), $a_0=5.38$ Å (Si), and $a_0=3.53$ Å (C).

The results of our *ab initio* calculations for SiC and for the pure elements Si and C are listed in Table I. We compare them with other *ab initio* calculations for Si (Ref. 3) and

TABLE I. Comparison of first-principles stacking-fault energies $\gamma_{\mathrm{ISF/ESF}}$ for different group-IV materials with other theoretical or experimental data available. The energies are in mJ/m^2.

		This work	Chou *et al.* (Ref. 3)	Experimental	ANNNI (Ref. 20)
Si	ISF	38	33	69[a]	47
	ESF	20	26	60[a]	36
C	ISF	318	—		300
	ESF	254	—	279[b]	253
SiC	ISF	−3.4	—		14
	ESF	−28	—	2.5[c]	−6

[a] Föll and Carter (Ref. 21).

[b] Pirouz *et al.* (Ref. 22).

[c] Maeda *et al.* (Ref. 23) for $6H$.

experimental data[21–23] as well as with the ANNNI calculations by Denteneer[20] for all three materials. The error in the total energy resulting from the finite plane-wave basis set and the Brillouin-zone sampling by a very limited number of **k** points can be estimated to be about 0.001 eV per atom pair. This results in possible relative errors of 10% (ESF) and 20% (ISF) for Si, 4% for diamond and 25% (ESF) for SiC. In the case of the ISF in SiC, the formation energy approaches the numerical accuracy.

The overall agreement concerning the magnitude of the formation energies is quite reasonable. In the case of Si, the absolute values from both *ab initio* calculations are somewhat smaller than the experimental ones. A more accurate quantity might be defined by the ratio of intrinsic and extrinsic stacking-fault energies, which can be accessed experimentally on one sample.[21] With 1.9 ± 0.6 this value is overestimated in our calculation compared to the experimental value of about 1.15 ± 0.09. For diamond, the stacking-fault energies are considerably larger than for silicon and the relative errors naturally smaller. Experimentally, the stacking-fault energy for C was determined by Pirouz *et al.*[22] with 279 ± 41 mJ m^{-2}, without distinguishing between ESF and ISF. Both of the calculated values are within the error of the experimental ones, and also the mean value of the calculated values of 286 mJ m^{-2} compares well with this value. Nevertheless, the agreement between the calculated stacking-fault energies with the experimental values is quite good taking into consideration the complicated procedures to extract such energies experimentally.

Common for Si and C is that their stacking fault energies are definitely positive, which is in agreement that polytypes of these materials are not observed under ambient conditions. In the limit of pure-covalent bonding they crystallize within the diamond structure. For SiC on the other hand, we find negative values for both ISF and ESF. However, since the result for the ISF approaches the numerical accuracy in this case, it should be taken with care. But considering the common polytypes 6*H* and 4*H*, the ESF should play a more important role since its stacking sequence is closer to the corresponding bulk stacking sequences than that of the ISF. The energy of the ESF is definitely negative and therefore causes the cubic zinc-blende polytype 3*C* not to be the dominant structure among the polytypes. Comparing the results for SiC with experimental data, Maeda has found 2.5 ± 0.9 mJm^{-2}.[23] However, this value was obtained for stacking-faults in a 6*H* polytype and a temperature of about 1600° C. Since 6*H* is preferred over 3*C* at this temperature, a positive sign of the stacking-fault energy is expected.

The accuracy of our total-energy calculations for the stacking faults in the critical case of SiC is characterized in Table II by the comparison of different ANNNI models. Their parameters are derived from various different total-energy calculations.[4,13,19,24] The stacking-fault energies are derived from expressions (2). From the total energies in a previous paper of ours[13] but also from those of other authors[4,18,24] we have calculated the parameters of the ANNNI model including next-nearest- and third-nearest-neighbor interactions. First, we observe that the interactions between third-nearest neighbors play only a minor role. Second, we see that in our calculations both of the stacking-fault energies are small, but definitely negative. The results compare very well with the data of Cheng, Heine, and Needs.[18] For the other two data sets, only $\gamma_{\rm ESF}$ is negative and also much smaller, whereas $\gamma_{\rm ISF}$ is of the same magnitude but possesses the opposite sign.

TABLE II. ANNNI model and stacking-fault energies for SiC. The interaction parameters J_i are in meV/Si-C pair, the energies $E_{\rm I/ESF}$ are also given in meV. The stacking-fault energies $\gamma_{\rm ISF/ESF}$ are obtained by normalizing the values with the area of the cell perpendicular to the stacking direction. They are given in mJ/m^2.

	2nd NN	3rd NN	(Ref. 4)	(Ref. 24)	(Ref. 18)
J_1	0.86	1.18	4.35	4.80	2.33
J_2	−2.34	−2.34	−2.57	−2.93	−3.49
J_3		−0.32		−0.45	0.25
$\Delta E_{\rm ISF}$	−5.90	−5.90	7.12	5.68	−3.64
$\Delta E_{\rm ESF}$	−15.24	−16.53	−3.16	−7.84	−16.60
$\gamma_{\rm ISF}$	−11.8	−11.8	13.8	11.1	−7.1
$\gamma_{\rm ESF}$	−30.6	−33.2	−6.1	−15.4	−32.3

For the faulted structures, the Hellmann-Feynman forces are calculated in the neighborhood of the faults and are optimized simultaneously with the electronic structure optimization. In Table III we present the calculated vertical deviations from the equilibrium positions determined by the cubic structures for Si, C, and SiC. From the point of symmetry, the deviations in Si and C add up to zero, whereas this is not necessarily the case in SiC. In case of the ESF, the movement of the silicon atoms is as follows: The vertical bond length of the two double layers where the stacking direction changes is stretched somewhat (this holds also for the ISF) and the vertical bond length of the added layer in between is shortened. The lateral bond lengths to the added layer mainly remain unchanged. The deviations for diamond are very

TABLE III. Vertical deviations in the faulted structures from the atomic positions in the unfaulted cubic structure (in 10^{-3}Å) for Si, C, and SiC. The stacking in the unit cells used for the optimization is indicated by the atomic positions in the $(11\bar{2})$ plane. In case of SiC filled (open) circles indicate Si (C) atoms. Six (four) atomic layers around the additional (missing) *A* bilayer are allowed to relax for the ESF (ISF).

ESF			Si	C	SiC	ISF			Si	C	SiC
		○						○			
		●						●			
	○						○		+6.7	+6.8	+4.2
	●						●		−1.7	+0.7	+0.8
○			+5.0	+4.0	+4.8			○	+1.7	−0.7	+1.2
●			−8.1	−8.6	−0.5			●	−6.7	−6.8	−0.7
	○		−4.1	−7.4	−1.1		○				
	●		+4.1	+7.4	−1.9		●				
		○	+8.1	+8.6	+4.3	○					
		●	−5.0	−4.0	+0.2	●					
	○										
	●										
C	A	B				A	B	C			

similar and of the same magnitude (somewhat larger anyway, according to a scaling with the lattice constant) and sign as for silicon.

For the ESF the situation in SiC is similar, even if the atoms move partially in the same direction. A major difference, however, is the tiny stretching of the vertical bond of the added layer. Since all three vertical bond lengths are stretched, the lateral ones have to be shortened. This phenomenon is the same as observed for the hexagonal polytypes of SiC.[13,25] Furthermore, the mean deviation, or more strictly, the mean value of the magnitude of all deviations, for SiC is only about 35% of the mean deviation for Si in both cases, ESF and ISF. This implies that the strain on the bonds in SiC caused by the faults can be released much more easily than in Si or C, or, that there is not as much strain as in Si or C.

Finally, we investigate the electronic structure for the ESF and ISF, but only for SiC because of the energetical favorization. We compare it with that of ideal zinc-blende SiC to determine possible defect states within the fundamental gap due to the stacking faults. To determine the projected band structure of the perfect crystal in the plane perpendicular to the cubic [111] direction, we have calculated the bands in an extended hexagonal unit cell. The eigenvalues for the faulted structures are plotted along high-symmetry lines in the two-dimensional hexagonal Brillouin zone together with the projected band structure of the ideal structure in Fig. 2. In agreement with the enlargement of the indirect energy gaps in the hexagonal polytypes, defect-related bound states appear only close to the band edges. The occupied defect bands can be distinguished from the perfect bands only for the ISF in the region between Γ and M, and partially also between M and K. At the Γ point, we find occupied defect states about 23 meV slightly above the valence-band maximum (VBM) for both structures. This is near the calculated natural valence-band offset of 21 meV between $6H$ and $3C$ SiC.[26] On the other hand, the situation close to the VBM is similar to the case of pure Si.[3] The conduction-band minimum (CBM) and therefore the gap energy is not lowered by the stacking faults as expected, since from all polytypes $3C$ has the smallest gap. However, for the ISF a rather pronounced defect-state band is observed around the K point. It could be related to the pure hexagonal stacking around the faults: From the $2H$ polytype we know that for pure hexagonal stacking the conduction-band minimum at the K point of the hexagonal Brillouin zone comes remarkably down in energy.

In conclusion, we have performed first-principles calculations of the properties of intrinsic and extrinsic stacking faults in cubic Si, C, and SiC. The agreement of the stacking fault energies with other theoretical and experimental data is reasonable. In contrast to Si and C, we find negative stacking fault energies for SiC, indicating the favoring of more hexagonal polytypes over zinc-blende SiC. The defect states lower the energy gap by only about 20 meV, which is comparable to the band offset of $6H$ SiC to $3C$ SiC.

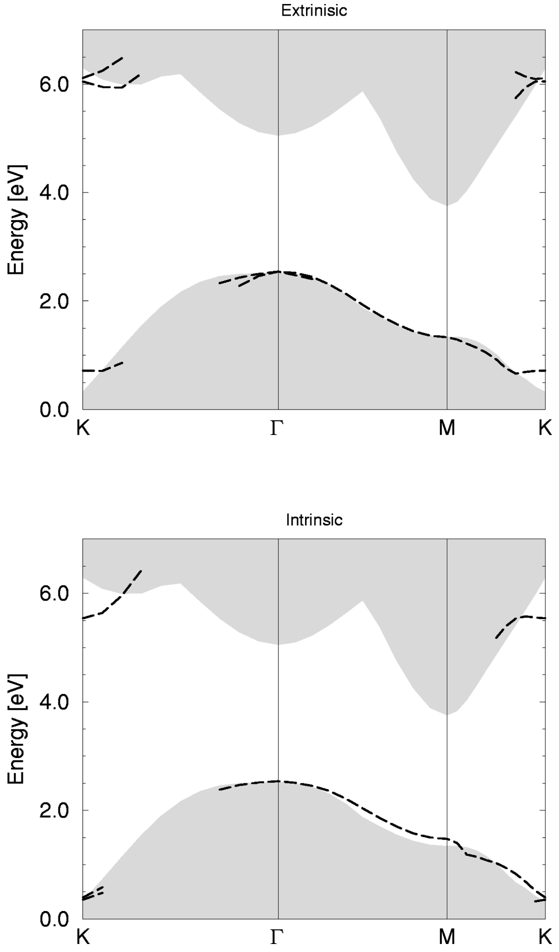

FIG. 2. Electronic structures for extrinsic (upper) and intrinsic (lower) stacking faults in SiC. The shaded area corresponds to the band structure of the perfect crystal projected onto the two-dimensional Brillouin zone of an ideal (111) plane. The defect bands are marked with dashed lines. Bulk and supercell band structures are aligned using the corresponding electronic potentials.

This work was supported by the Sonderforschungsbereich 196 (Project No. A08) of the Deutsche Forschungsgemeinschaft.

---

[1] P. Pirouz and J. W. Yang, Ultramicroscopy **51**, 189 (1993).

[2] P. Pirouz and P. M. Hazzledine, Solid State Phenom. **35-36**, 183 (1994).

[3] M. Y. Chou, M. L. Cohen, and S. G. Louie, Phys. Rev. B **32**, 7979 (1985).

[4] P. J. H. Denteneer, in *Atomic Scale Calculations in Materials Science*, edited by J. Tersoff, D. Vanderbilt, and V. Vitek, MRS Symposia Proceedings No. 141 (Materials Research Society, Pittsburgh, 1989), p. 343.

[5] C. Cheng, R. J. Needs, and V. Heine, J. Phys. C **21**, 1049 (1988).

[6] P. Hohenberg and W. Kohn, Phys. Rev. **136**, B864 (1964).

[7] W. Kohn and L. Sham, Phys. Rev. **140**, A1133 (1965).

[8] D. M. Ceperley and B. J. Alder, Phys. Rev. Lett. **45**, 566 (1980).

[9] J. P. Perdew and A. Zunger, Phys. Rev. B **23**, 5048 (1981).

[10] G. B. Bachelet, D. R. Hamann, and M. Schlüter, Phys. Rev. B **26**, 4199 (1982).

[11] L. Kleinman and D. M. Bylander, Phys. Rev. Lett. **48**, 1425 (1982).

[12] B. Wenzien, P. Käckell, and F. Bechstedt, Surf. Sci. **307-309**, 989 (1994).

[13] P. Käckell, B. Wenzien, and F. Bechstedt, Phys. Rev. B **50**, 17 037 (1994).

[14] A. Scholze, W. G. Schmidt, and F. Bechstedt, Phys. Rev. B **53**, 13 725 (1996).

[15] R. Car and M. Parrinello, Phys. Rev. Lett. **55**, 2471 (1985).

[16] R. Stumpf and M. Scheffler, Comput. Phys. Commun. **79**, 447 (1994).

[17] D. J. Chadi and M. L. Cohen, Phys. Rev. B **8**, 5747 (1973).

[18] C. Cheng, V. Heine, and R. J. Needs, J. Phys.: Condens. Matter **2**, 5115 (1990).

[19] F. Bechstedt, P. Käckell, A. Zywietz, K. Karch, B. Adolph, K. Tenelsen, and J. Furthmüller, Phys. Status Solidi B **202**, 35 (1997).

[20] P. J. H. Denteneer and W. v. Haeringen, Solid State Commun. **65**, 115 (1988).

[21] H. Föll and C. Carter, Philos. Mag. A **40**, 497 (1979).

[22] P. Pirouz, D. J. H. Cockayne, N. Sumida, P. Hirsch, and A. R. Lang, Proc. R. Soc. London, Ser. A **386**, 241 (1983).

[23] K. Maeda, K. Suzuki, S. Fujita, M. Ichihara, and S. Hyodo, Philos. Mag. A **57**, 573 (1988).

[24] K. Karch, G. Wellenhofer, P. Pavone, U. Rössler, and D. Strauch, in *Proceedings of the 22nd International Conference on the Physics of Semiconductors, Vancouver, 1994*, edited by D. Lockwood (World Scientific, Singapore, 1995), p. 401.

[25] A. Bauer, J. Kräußlich, L. Dressler, P. Kuschnerus, S. Wolf, K. Goetz, P. Käckell, J. Furthmüller, and F. Bechstedt, Phys. Rev. B **57**, 2647 (1998).

[26] P. Käckell, B. Wenzien, and F. Bechstedt, Phys. Rev. B **50**, 10 761 (1994).